A study of the past dynamics of comet 67P/Churyumov-Gerasimenko with Fast Lyapunov Indicators

Massimiliano Guzzo, Elena Lega

▶ **To cite this version:**

Massimiliano Guzzo, Elena Lega. A study of the past dynamics of comet 67P/Churyumov-Gerasimenko with Fast Lyapunov Indicators. 2015. hal-01113202v1

HAL Id: hal-01113202

https://hal.science/hal-01113202v1

Preprint submitted on 4 Feb 2015 (v1), last revised 26 Nov 2020 (v2)

HAL is a multi-disciplinary open access archive for the deposit and dissemination of scientific research documents, whether they are published or not. The documents may come from teaching and research institutions in France or abroad, or from public or private research centers.

L'archive ouverte pluridisciplinaire **HAL**, est destinée au dépôt et à la diffusion de documents scientifiques de niveau recherche, publiés ou non, émanant des établissements d'enseignement et de recherche français ou étrangers, des laboratoires publics ou privés.

Preprint, 04 february 2015

A study of the past dynamics of comet 67P/Churyumov-Gerasimenko with Fast Lyapunov Indicators

Massimiliano Guzzo[1], Elena Lega[2]

Abstract
Comet 67P/Churyumov-Gerasimenko is the target of the Rosetta mission. On the base of backward numerical integrations of a large set of fictitious comets whose initial conditions are obtained from small variations of the orbital parameters of 67P, and the analysis of suitable chaos indicators, we detect the phase–space structure of the past close encounters of the comet with Jupiter. On the base of these computations we find that the comet could have being injected in the inner Solar System from distances larger than 100 AU from the Sun with a probability of 60 per cent in the past 150000 years and could have passed under the Jupiter's Roche limit with a probability of about 4 percent in the same time interval.

[1] *Università degli Studi di Padova, Dipartimento di Matematica, Via Trieste, 63 - 35121 Padova, Italy, guzzo@math.unipd.it*
[2] *Université de Nice Sophia Antipolis, CNRS UMR 7293, Observatoire de la Côte d'Azur, Bv. de l'Observatoire, C.S. 34229, 06304 Nice cedex 4, France, elena.lega@oca.eu*

Contents

1 **Introduction** 1
2 **The Fast Laypunov Indicator analysis of close encounters** 2
3 **Results** 3
4 **Conclusions** 8
References 8

1. Introduction

The past dynamics of comet 67P/Churyumov-Gerasimenko becomes rapidly uncertain for increasing time–intervals because of its several close encounters with Jupiter: very small errors in the initial conditions, as well as in the parameters determining the forces model, can be amplified at any close encounter with Jupiter, or other planets. This behaviour is typical of the comets of the so called Jupiter family (see, for example, [16, 17, 11, 12, 23]). Specifically, for comet 67P/Churyumov-Gerasimenko, a sequence of deep close encounters with Jupiter (the last deep one occurred in 1959, see [3, 2, 4]) limits the precision of its orbit computation to few centuries (see [7, 18]). This uncertainty is annoying, since, a detailed knowledge of the long–term past dynamics of the comet would be a useful complement to some of the outcomes of the experiments of the Rosetta mission, see [1, 22].

In this paper we perform an analysis of the dynamics of comet 67P with a technique developed in the last decade in the framework of hyperbolic dynamical systems [6, 5, 13, 14], recently modified to analyze close encounters in the three–body problem approximation ([9], see also [19, 8, 9, 10]). In this study we suitably adapt the technique to study the close encounters of a real body with a Planet using a model of the Solar System compatible with the JPL DE431 ephemerides, which in particular takes into account the gravitational interactions with the Planets and with the four most massive asteroids, general relativity and the non–gravitational cometary forces modeled by the so-called standard model of cometary dynamics.

Though it is not possible to determine the precise orbit of an individual object performing multiple close encounters with a planet in a fixed time interval $[0,T]$, we determine the phase–space structure of all the initial conditions whose orbits have close encounters in $[0,T]$. In fact, on suitably chosen sections of the phase-space, the structure of the close encounters appears as the ridges of a chaos indicator, precisely the Fast Lyapunov Indicator [19, 8], modified by filtering the contributions due to any single close encounter [9]. The skeleton of this structure is represented by the collision manifold, that is the set of initial conditions whose orbits have a collision with the barycenter of the planet in $[0,T]$. Since we do not know the initial conditions of the comet with infinite precision, we do not know its exact localization relatively to the structure of close encounters, but we have hints about all the typical

dynamics which are compatible with the uncertainties in the orbital determination. Profitting of the knowledge of the collision manifolds, these typical dynamics can be analyzed with statistical purposes by changing the initial conditions only on a one dimensional direction transverse to the collision manifold, rather than through the sixth dimensional confidence ellipsoid, with considerable saving of CPU time: a sampling of N initial conditions with our method corresponds to a sampling of N^6 initial conditions in the 6th dimensional space of initial positions and velocities of the comet. Moreover, the topological coherence of the detected structures provides an indication of good control of round-off approximations. Our analysis can be performed on any Jupiter family comet, we treat the 67P/Churyumov–Gerasimenko as a case study, since as an outcome of the Rosetta mission we have a particularly good determination of the orbital parameters and of the parameters A_1, A_2, A_3 entering the definition of the standard model of cometary dynamics. Our results, reported in Section 3, are specific to comet 67P, and cannot be exported to other Jupiter families comets without specific analysis.

For 67P/Churyumov Gerasimenko, we find in particular that within the uncertainties for the initial conditions provided by the JPL ephemerides system, the comet could have visited in the past 150000 years regions distant more than 50 AU from the Sun with a probability of 72 per cent (and regions distant more than 100 AU from the Sun with a probability of 60 per cent), before being injected in the inner Solar system, and could have passed under the Jupiter Roche limit with a probability of about 4 percent. Are these results indicating a certain dynamical origin for the comet? We will return to these delicate question in the Conclusions Section.

The paper is organized as follows. In Section 2 we describe the Fast Lyapunov Indicator method for the computation of the structure of close encounters; in Section 3 we report the results obtained for comet 67P/Churyumov-Gerasimenko; in Section 4 we provide conclusions.

2. The Fast Laypunov Indicator analysis of close encounters

We refer to the dynamics of comet 67P as the dynamics obtained from the initial conditions provided by the JPL ephemerides system with a numerical integration of the forces model described in [24], Section 1.2, accounting for the gravitation of the planets, from Mercury to Pluto; the most important post-Newtonian contributions from general relativity; the non gravitational forces modeled by the standard-model of cometary dynamics [20], (with values of the parameters A_1, A_2, A_3 provided by the JPL ephemerides system); the gravitational interaction with four asteroids (Ceres, Pallas, Vesta, Hygea). The small–scale analysis which we consider is sensitive to all these contributions in different extents; other effects, such as additional asteroids, have very little impact (see Section 3, figure 3), while the non-sphericity of the Sun, does not seem to have any relevance. Our analysis is based on the numerical integrations of the orbits of hundreds of thousands of fictitious comets, whose initial conditions are obtained by slightly changing the initial conditions of comet 67P. We denote by $\xi = (r, \dot{r}) = (x, y, z, \dot{z}, \dot{y}, \dot{z})$ the vector of Cartesian components of the position r and velocity $\dot{r}$ of a fictitious comet in a heliocentric reference frame, and by

$$\dot{\xi} = F(\xi, t) \tag{1}$$

the first order differential equations defining the dynamics of the comet. For any initial condition ξ_0 (the initial condition of the comet will be denoted by ξ_*) at a given reference epoch[1], we numerically integrate backward equations (1) as well as its variation equations:

$$\dot{w} = \left[\frac{\partial F}{\partial \xi}(\xi(t), t) \right] w \tag{2}$$

with some initial conditions $w(0) \in \mathbb{R}^6$ ($\frac{\partial F}{\partial \xi}(\xi, t)$ denotes the Jacobian matrix of $F(\xi, t)$; $\xi(t)$ denotes the solution of (1) with initial conditions $\xi(0) = \xi_0$). The growth of the norm of the tangent vector $\|w(t)\|$ with time, where $w(t)$ is the solution of the variational equations with initial conditions $(\xi(0), w(0)) = (\xi_0, w_0)$, is a well known method of characterizing the divergence of orbits with initial conditions very close to ξ_0. Even if the traditional technique of computation of characteristic Lyapunov exponents, that is of quantities:

$$\lambda(\xi_0, w_0) = \lim_{t \to +\infty} \frac{1}{t} \log \|w(t)\|,$$

is not suitable for the case of close encounters (the equations are singular and orbits can escape from the Solar System), all the fictitious comets with initial conditions close to ξ_* are characterized by some strong growth of $\|w(t)\|$. As a matter of fact, the growth of tangent vectors due to close encounters has analogies with the growth of tangent vectors for initial conditions close to the stable and unstable manifolds of hyperbolic orbits (see [8]), a case which has been analyzed in detail in [9]. In this analogy, the stable manifold is identified with the collision manifold, that is the set of initial conditions whose orbits have a collision with the barycenter of the planet in $[0, T]$. As a consequence, the distance of an initial condition from an initial condition on a collision orbit is well characterized by a dynamical indicator obtained from the Fast Lyapunov Indicator. In [9] we have modified the indicator with the introduction of a window function whose effect is that of filtering out all the contributions to the indicator which are not due to close encounters. Precisely, the Fast Lyapunov Indicator of ξ_0 modified with a window functions $u(\xi)$, at time T is defined by ([9], and also [10]):

$$FLI_u(\xi_0, w_0, T) = \int_{T_0}^{T} u(r(t) - r_j(t)) \frac{w(t) \cdot \dot{w}(t)}{\|w(t)\|^2} dt, \tag{3}$$

where $\xi(t), w(t)$ are the solutions of equations (1) and (2) with initial conditions $(\xi(0), w(0)) = (\xi_0, w_0)$, and $r_j(t)$ denotes

[1] In our computations the initial reference epoch is fixed to 11-14-2014.

the orbit of the j–th planet, which is Jupiter for Jupiter–family comets. A suitable choice for u (see [9]), obtained from the so–called Hanning window, is:

$$u(r) = \begin{cases} 1 & \text{if } |r| \le \frac{\rho}{2} \\ \frac{1}{2}[\cos((\frac{|r|}{\rho} - \frac{1}{2})\pi) + 1] & \text{if } \frac{\rho}{2} < |r| \le \frac{3\rho}{2} \\ 0 & \text{if } |r| > \frac{3\rho}{2} \end{cases} \quad (4)$$

where ρ is a parameter, which will be chosen of the same order of the Hill radius. The FLI defined in (3) measures the chaotic effects on an orbit due to the close encounters with Jupiter in the time interval $[T_0, T]$. By computing this modified Fast Lyapunov Indicator, hereafter simply denoted by FLI, on two dimensional surfaces of different initial conditions, the collision manifold appears as the ridges of the FLI, and the initial conditions close to the top of a ridge, that is initial conditions with a significant FLI value, have close encounters which give rise to significant divergence of their nearby orbits. Moreover, since the FLI rapidly decreases by increasing the distance from the top of the ridge (see [9]), the collision manifold is sharply identified and the distribution of FLI values provides the topological structure of close encounters. We remark that a property of the ridge structures of close encounters is its stability with respect to small variations of the forces model, while the individual orbits are not. In fact, even if a small change of the model can produce a big change to an orbit with initial conditions ξ_0, very close to ξ_0 there will be initial conditions with dynamics similar to the previous one, so that the ridges will be only slightly moved, see Section 3 for examples.

3. Results

FLI detection of the collision manifold. We obtain sharp representations of the structure of close encounters by computing the FLI for refined grids of initial conditions in the two–dimensional surface of the space of the Cartesian coordinates and velocities:

$$\Sigma = \{(x, y, z, \dot{z}, \dot{y}, \dot{z}) : \ (x, y, z, \dot{y}) = (x_*, y_*, z_*, \dot{y}_*), \\ \text{and } \ |\dot{x} - \dot{x}_*| < \sigma \ \ |\dot{z} - \dot{z}_*| < \sigma\} \quad (5)$$

where $(x_*, y_*, z_*, \dot{x}_*, \dot{y}_*, \dot{z}_*)$ is the initial condition of comet 67P provided by the JPL Horizon ephemerides system, and $\sigma = \sigma_1 = 10^{-6}$ or $\sigma = \sigma_2 = 10^{-7}$ AU/day. The values of σ_1 and σ_2 have been chosen according to the errors on the determination of the initial conditions, and according to the stability of the detected structures with respect to small changes of the forces model. The FLI (3) is computed using the same initial tangent vector $w(0)$; the numerical integration of the variational equations is performed with negative time steps from the initial epoch of 11-14-2014, here identified by $t = 0$, while T_0 is set just prior to the deep close encounter of 1959 (which is experienced by all the initial conditions which we consider), and different values of $T < T_0$. Then, the FLI is represented using a color scale, providing this way snapshots of the structure of the close encounters occurring in the time interval $[T, T_0]$. The results of the FLI computations are represented in figure 1. Since in figure 1 the yellow color represents the higher values of the FLI, the top of the ridges of the FLI appear as yellow curves[2], with many typical lobes visible on the zoomed out picture obtained for $\sigma = 10^{-6}$. All these curves pinpoint the set of initial conditions whose orbits have had past close encounters with Jupiter, in addition to the deep close encounter of 1959. By increasing $|T|$, ridges corresponding to other close encounters appear in the pictures: since the ridges do not intersect, it is easy to understand how the ridges are expected to fill densely the picture by increasing further the time $|T|$.

Within a ridge, the depth of all these encounters is related to the FLI value: to detect the orbits with deeper and deeper close encounter one needs to zoom in the ridge, see figure 2. The ridges detected in figure 1 are stable by small changes of the model, even if the individual orbits are not. This is shown in figure 3, where we compare the detection of the ridge structures and the individual orbits of fictitious comets computed with two different forces model: model (A), corresponding to the forces model described in Section 1, which includes also the four most massive asteroids, and model (B) corresponding to model (A) with seven additional asteroids (Euphrosyne, Eunomia, Davida, Interamnia, Cybele, Juno and Psyche). On the top panels we represent the value of the FLI computed for many initial conditions with $|T| = 400$ yrs, by numerically integrating the model (A) of the Solar system (black line), and model (B) (blue line). All the initial conditions have $x_0 = x_*, y_0 = y_*, z_0 = z_*, \dot{x}_0 = \dot{x}_*, \dot{y}_0 = \dot{y}_*$ and $|\dot{z}_0 - \dot{z}_*| \le 10^{-7}$ AU/day (top–left panel). The FLI profile represented in the top panels provides one-dimensional sections of the ridges represented in figure 1, left-panels. From the top–left panel of figure 3 we appreciate that the FLI profile of the black and blue curves are very similar, and to appreciate the differences we need to represent a zoom (top–right panel). In the zoom, we clearly appreciate that for both models a peak of the FLI is detected, and the effect of the 7 additional asteroids moves the peak of only 50 centimeters/day! The computation of the ridges is very stable with respect to the small perturbation due to the seven additional asteroids, even if individual orbits are not: from the bottom panels we appreciate that two sample orbits obtained from the same initial conditions, but integrated with the two models, are well separated at 450 years backward.

Cumulative dynamical effect of close encounters. We here discuss the cumulative effect on the dynamics due to the several close encounters of the comet with Jupiter. In particular, we consider the statistics of the passages of the comet below the so called Roche limit (where the comet can disintegrate due to Jupiter's tidal forces), and the measure of the past maximum distance from the Sun reached in some interval $[T, T_0]$.

First, we represent such maximum distance D for a large set

[2] We remark that, due to the use of the window function u in the computation of the FLI, the ridges detected this way should not be confused with the so-called Lagrangian coherent structures used for the analysis of time–dependent ODEs, see for example [15, 21], in fluid dynamics contexts.

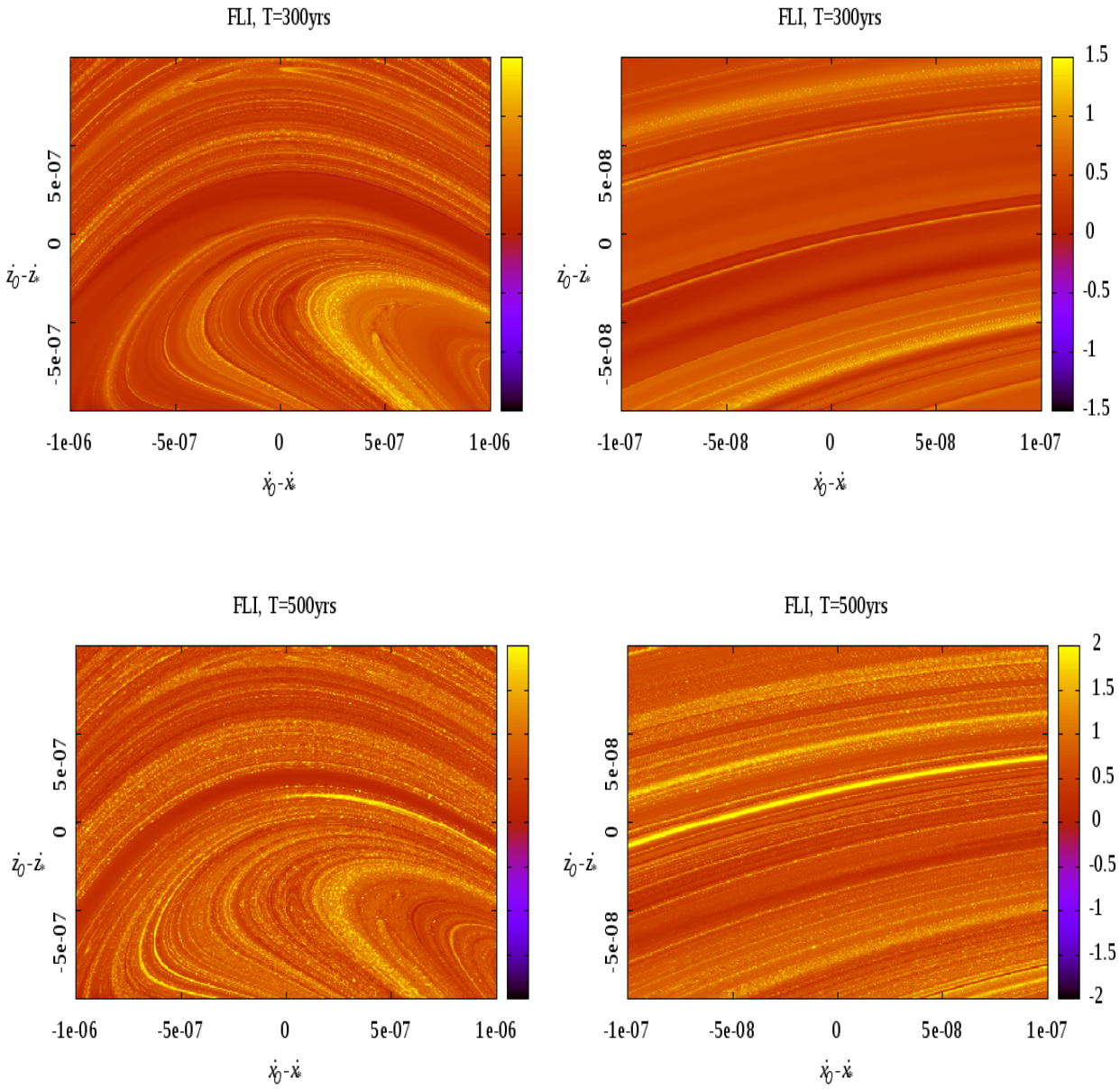

Figure 1. Representation of the FLI (3) *computed a grid of* 500×500 *initial conditions regularly spaced on* $(\dot{x}, \dot{z})$ *(the axes on the picture, which represent* $(\dot{x}_0 - \dot{x}_*, \dot{z}_0 - \dot{z}_*)$*–the other initial conditions are* $x_0 = x_*, y_0 = y_*, z_0 = z_*, \dot{y}_0 = \dot{y}_*$*), computed for* $|T| = 300$ *yrs (top panels) and* $|T| = 500$ *yrs (bottom panels); the left panels are a zoom of the right ones. The FLI is reported using a color scale, such that the highest FLI values correspond to the yellow color. In such a way, the yellow curves on the picture correspond to the ridges of the FLI indicator, and pinpoint the set of initial conditions whose orbits have past close encounters with Jupiter, additional with respect to the deep close encounter of 1959.*

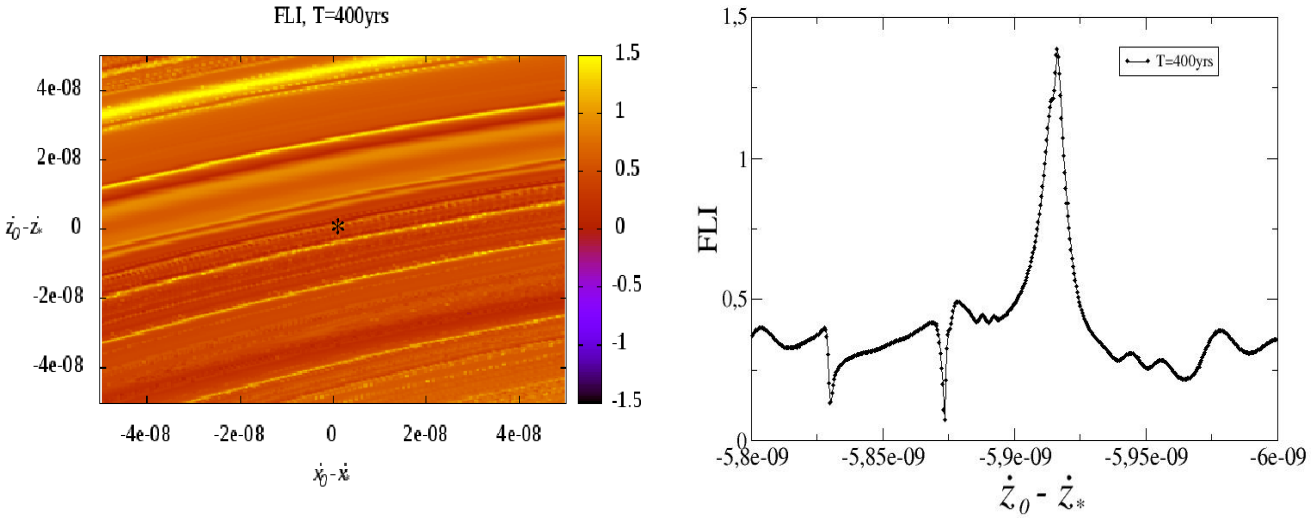

Figure 2. Zooming in selected ridges *of the FLI. On the left panel, we select a faint ridge to zoom in, marked with an asterisk. Since the ridges are almost parallel to the $\dot{x}$ axis, we can suitably represent their 1-dimensional section by computing again the FLI on many more initial conditions close to the ridge, but having the same value of $\dot{x}$. The result of the 1-dimensional FLI computation is represented in the right panel: zooming in the ridge we better detect its amplitude, and initial conditions having deeper encounters. The integration time is $|T| = 400$ yrs.*

of fictitious comets with initial conditions in Σ, for $|T| = 500$ yrs (figure 4, top panels). The curves of the largest maximum distance are clearly correlated to the ridges of the FLI (compare with figure 1), but at a first glance, the zoomed out picture (top-left panels) seems to reveal that only few initial conditions on a selected ridge have D larger, for example, than 15 AU (corresponding to orange in the picture). By zooming in around the origin (figure 4, top–right panel), we understand that the top of one of the ridges is uniformly characterized by initial conditions with maximum distances larger than 15 AU. Therefore, on the one hand, to detect correctly the probability of finding orbits with large maximum distances we need to zoom in the ridges, on the other hand, to compute such probabilities we are allowed to fix one additional initial condition, such as $\dot{x}_0 = \dot{x}_*$.

In the bottom panels of figure 4 we represent the computation of the maximum distance D for 10000 initial conditions, obtained from ξ_* by changing only $\dot{z}_*$, for $|T| = 1000$ yrs and $|T| = 2000$ yrs (a cut-off distance of 100 AU has been also introduced; the integrations are not stopped even if the comet passes under the Roche limit): by increasing the integration time, we obtain a significant increase of the number of ridges characterized by a large value of D. Due to the sharp oscillations of D with respect to $\dot{z}_0$, only a statistical interpretation of these results is possible. In figure 5 we represent the statistics about the time evolution of D for a sample of $N = 1000$ fictitious comets, whose initial conditions regularly spaced on $\dot{z}_0$ in the interval $|\dot{z}_0 - \dot{z}_*| \leq 10^{-7}$ (the other initial conditions are the same as ξ_*). Due to our knowledge of the collision manifold, our one dimensional sampling of initial conditions is representative of a multi–dimensional sampling of N^6 elements. Precisely, for any time $|T|$ ranging from 0 to 150000 yrs, we report the percentages of fictitious comets whose maximum distance from the Sun has been smaller that 30 AU; between 30 and 50 AU; between 50 and 100 AU and larger than 100 AU. We also reporte the percentage passed under Jupiter's Roche limit. For figure 5, we appreciate a large probability for the comet of having being injected in the inner Solar System from large d istances from the Sun: from distances larger than 100 AU from the Sun with a probability of 60 per cent in the past 150000 years and, from distances larger than 50 AU from the Sun with a probability of 72 per cent. Moreover, the comet could have passed under the Jupiter's Roche limit with a probability of about 4 percent in the same time interval.

Details about the numerical integrations. All the numerical integrations have been performed in double precision with an integrator which we specifically designed for this experiment. The comet and all the planets are integrated at the same time, with individual integration steps performed with a well known 6th–order Runge-Kutta integrator, but the step-size is adjusted within the code to treat close encounters as follows: if the comet is outside 3/2 Hill radii of any planet, all the bodies are integrated with a step-size τ_0 of 2.4 hours; if the comet is at a distance from a Planet smaller that 3/2 Hill radii the integration step-size τ is reduced so that in modulus it is the smaller between $\tau_0/10, 10^{-8}d^2/GM, 10^{-5}/|\dot{r}|$, where d denotes the distance between the comet and the closest planet and GM the product of the gravitation constant G and the mass of that planet. The variational equations are integrated the same way. The results are stable by further reductions of the time step: by reducing all the time steps by a factor 10 on sample orbits, we do not notice differences in their orbits before and after

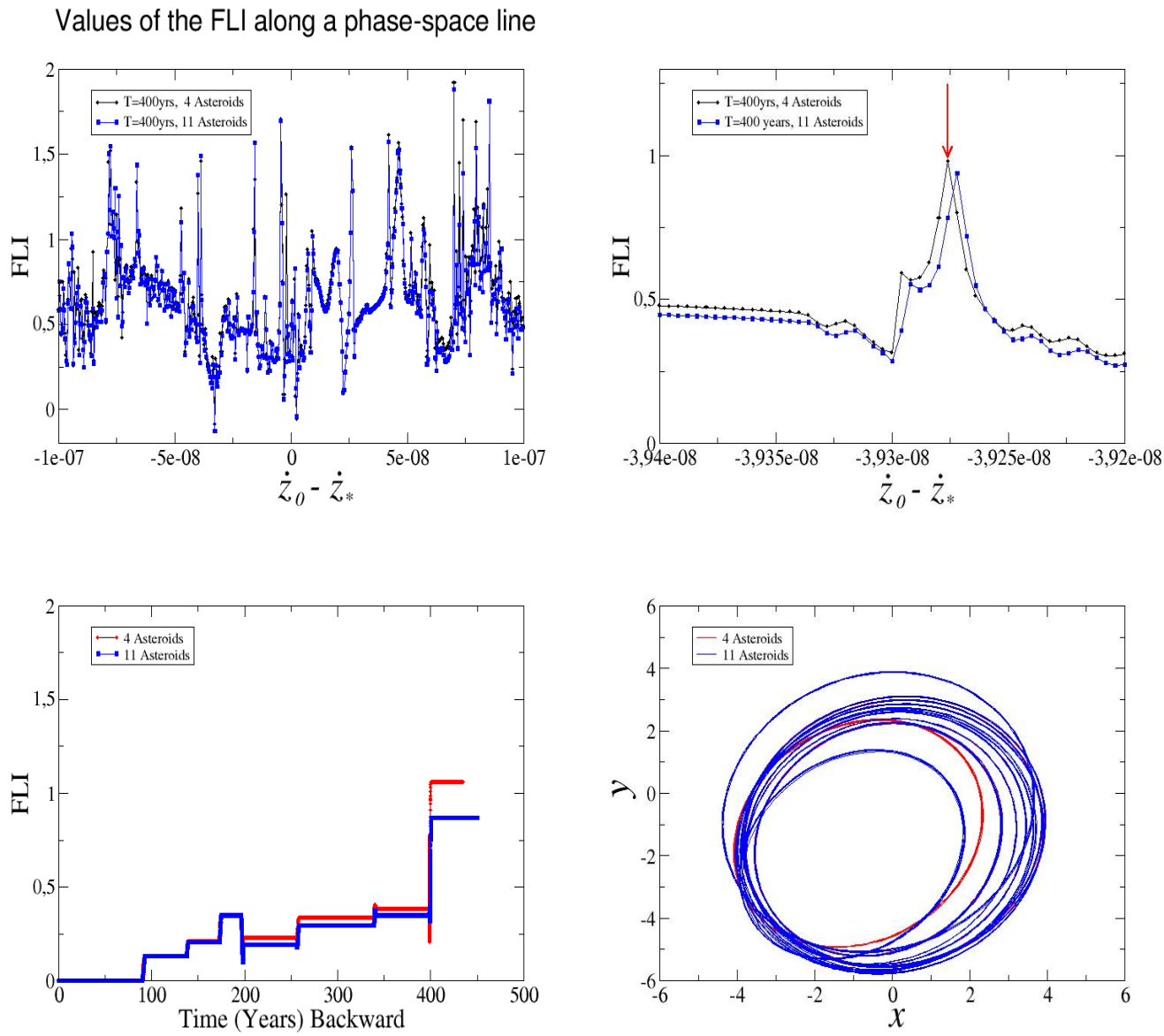

Figure 3. Effects of the small variations of the forces model to the ridge structure of close encounters and to individual orbits. *On the top panels we represent the value of the FLI computed for many initial conditions with* $|T| = 400$ *yrs, by numerically integrating the model of the Solar system including the four most massive asteroids (model (A), black line), and another model including seven additional asteroids (model (B), blue line). All the initial conditions have* $x_0 = x_*, y_0 = y_*, z_0 = z_*$, $\dot{x}_0 = \dot{x}_*, \dot{y}_0 = \dot{y}_*$ *and different* $\dot{z}_0 \sim \dot{z}_*$. *From the top–left panel we appreciate that the FLI profiles obtained with both models (A) and (B) are very similar, and to appreciate the differences we represent a sample zoom in the top–right panel. We clearly appreciate that for both models a peak of the FLI is detected, and the effect of the additional asteroids moves the peak of only* 50 *centimeters/day. On the bottom panels we represent instead the effect of the additional asteroids on the orbit with initial conditions corresponding to the top of the left-peak (marked with an arrow). In the bottom–left panel the FLI evolution for a time interval ranging from* 0 *to* 450 *years backwards is represented: the impulsive variations of the FLI occur at the close encounters: the very small difference in the two models changes the time of some close encounters, and this is amplified at the other close encounters. The close encounter occurring at* 400 *yrs backward determines the strong divergence of the two orbits, whose projection on the* $x - y$ *plane is represented in the bottom–right panel. Up to* 400 *years the two orbits are almost identical, but between* 400 *and* 450 *years backward the two orbits are well separated.*

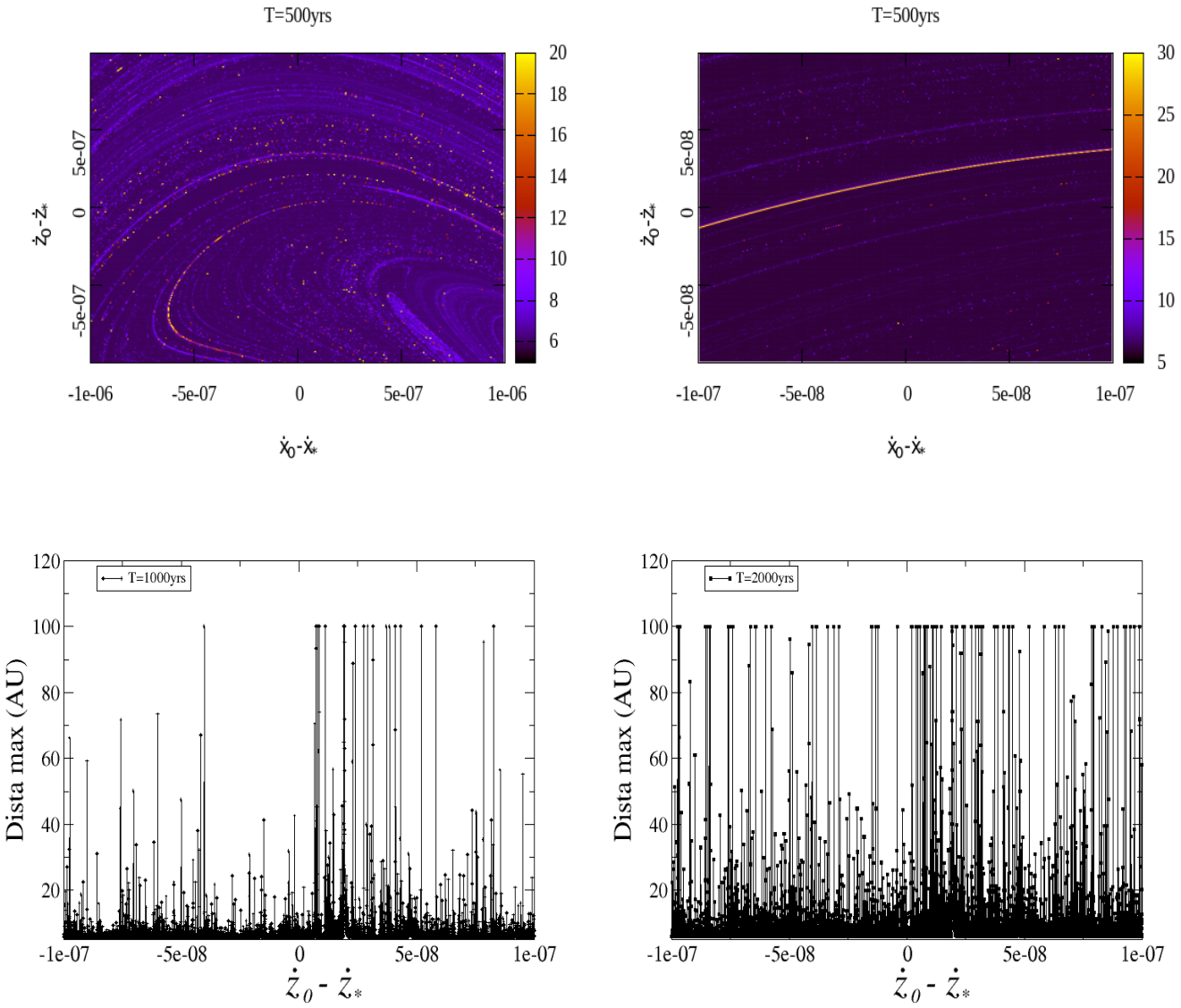

Figure 4. Representation of the maximum distance from the Sun *reached in the interval* $[T, T_0]$ *by orbits with initial conditions on a grid of* 500×500 *initial conditions regularly spaced on* $(\dot{x}, \dot{z})$ *(the axes on the picture, which represent* $(\dot{x}_0 - \dot{x}_*, \dot{z}_0 - \dot{z}_*)$*–the other initial conditions are the same of comet 67P), for* $|T| = 500$ *yrs (top panels). The color scale represents the maximum distance, so that the yellow means distances larger than 20 AU (top–left panel) or 30 AU (top-right panel). The top–right panel is a zoom of the top-left panel. The curves of the pictures are clearly correlated to the ridges of the FLI (see figure 1); the topology detected in the zoomed in picture indicates that we can continue the exploration by fixing the value of* $\dot{x}_0 = \dot{x}_*$*: in the bottom panels we represent the maximum distance from the Sun reached in the interval* $[T, T_0]$ *by 10000 orbits with all the initial conditions equal to* ξ_**, except for* $\dot{z}_0$*, and times* $T = 1000$ *(bottom–left panel) and* $T = 2000$ *(bottom–right panel).*

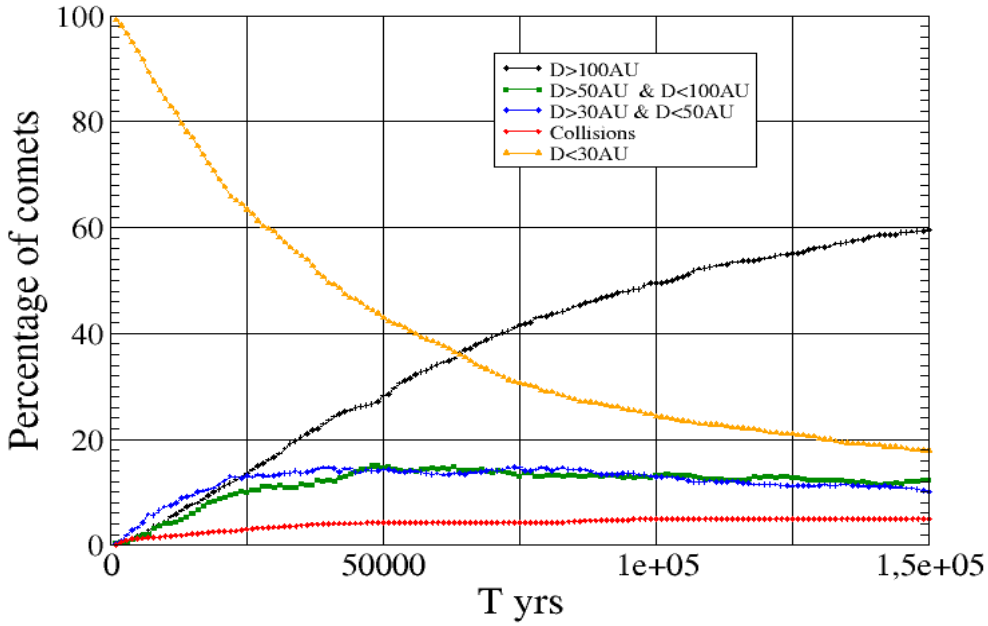

Figure 5. Statistical evolution of the maximum distance from the Sun *reached in the interval* $[T,0]$ *by orbits with initial conditions on a grid of 1000 initial conditions regularly spaced on* $\dot{z}_0$*, with* $|\dot{z}_0 - \dot{z}_*| \leq 10^{-7}$ *(the other initial conditions are the same as* ξ_**), up to* $|T| = 150000$ *yrs. Precisely, at any given value of the time* $|T|$*, we represent the percentage of comets whose maximum distance from the Sun in* $[T,0]$ *has been smaller than 30 AU, between 30 AU and 50 AU, between 50 and 100 AU, and larger than 100 AU. We also represent the percentage of fictitious comets passed under Jupiter's Roche limit.*

deep close encounters.

4. Conclusions

The computation of the FLI indicator on a large number of initial conditions provides us the knowledge of the collision manifold of the comet 67P/Churyumov-Grasimenko with Jupiter, as well as the structure of the close encounters which determine divergence of the orbits. On the base of these computations, we have been able to choose a direction which is transverse to the branches of the collision manifold. By computing the backward time evolution of many orbits with initial conditions along this direction, we obtained that a large fraction of them, corresponding to 60 per cent, have visited in the past 150000 years regions of the Solar System distant more than 100 AU from the Sun. Therefore, there is a strong dynamical link between these regions of the phase space and the present values of orbital parameters of the comet. Is this fact indicating a certain dynamical origin of the comet? The answer could be quite complex, as the paradgmatic case of comet Encke suggests. The first aspect to consider is the intimate nature of statistics, which is valid for many fictotious comets with orbital parameters very close to those of 67P, but does not apply on the single real object. The second aspect to consider concerns backward integrations of systems with dissipation. It is well known that strongly dissipative systems cannot be integrated backwards, for example when the initial condition is in some attractor, but this seems not to be the case of comet 67P, since dissipation is weak and acting mainly close to the perycenter; in any case this point should be further developed. The third aspect is of astronomical type, since it is generally accepted that the probability for a comet to transit from the Oort cloud to the Jupiter family (with forward integrations) is very small. For all these reasons, we think that our result could be used to understand the origin of the comet only in presence of additional knowledge, independent from dynamics.

Acknowledgments

We thank G.B. Valsecchi for a preliminary reading of our manuscript, and for a long discussion about the origin of comets. M. Guzzo gas been supported by the Italian project PRIN "Teorie geometriche e analitiche dei sistemi Hamiltoniani in dimensioni finite e infinite", and by the project CPDA149421/14 of University of Padova "New Asymptotic Aspects of Hamiltonian Perturbation Theory". The numerical computations have been done on the "Mesocentre SIGAMM" machine, hosted by the Observatoire de la Cote d'Azur.

References

[1] Altwegg K. et al., 67P/Churyumov-Gerasimenko, a Jupiter family comet with a high D/H ratio. Science, vol. 347, issue 6220, 2015.

[2] Belyaev N.A., Kresák L., Pittich E.M., Pushkarev A.N., Catalogue of Short-Period Comets, Veda, Bratislava, 1985.

[3] Carusi A., Kresák L., Perozzi E., Valsecchi G.B., Long-Term Evolution of Short-Period Comets, Hilger, Bristol, 1985.

[4] Carusi A., Kresák L. and Valsecchi G.B., Atlas of Dynamical Evolutions of Short–Period Comets. Formerly available on the World Wide Web at http://www.ias.rm.cnr.it/ias-home/comet/catalog.html, 1995.

[5] Froeschlé Cl., Guzzo M. and Lega E., Graphical Evolution of the Arnold Web: From Order to Chaos, Science, vol. 289, 5487, 2108-2110, 2000.

[6] Froeschlé Cl., Lega E. and Gonczi R., Fast Lyapunov indicators. Application to asteroidal motion. Celest. Mech. and Dynam. Astron., vol. 67, 41–62, 1997.

[7] Groussin O., Hahn G., Lamy P.L., Gonczi R. and Valsecchi G.B., The long-term evolution and initial size of comets 46P/Wirtanen and 67P/Churyumov–Gerasimenko, Mon. Not. R. Astron. Soc., vol. 376, 1399–1406, 2007.

[8] M. Guzzo M., E. Lega, On the identification of multiple close-encounters in the planar circular restricted three body problem." Monthly Notices of the Royal Astronomical Society, 428, 2688-2694, 2013.

[9] Guzzo M., E. Lega, Evolution of the tangent vectors and localization of the stable and unstable manifolds of hyperbolic orbits by Fast Laypunov Indicators, SIAM J. APPL. MATH., Vol. 74, No. 4, pp. 1058–1086, 2014.

[10] Guzzo M., E. Lega, Computation of transit orbits in the three-body-problem by Fast Lyapunov Indicators, to appear in the proc. of the XVII Ncas, Belgrade, 2014.

[11] Levison H. F., Duncan M. J., The long-term dynamical behavior of short-period comets. Icarus, vol. 108, no. 1, p. 18-36, 1994.

[12] Levison H. F., Duncan M. J., From the Kuiper Belt to Jupiter-Family Comets: The Spatial Distribution of Ecliptic Comets, 1997.

[13] M. Guzzo, E. Lega and C. Froeschlé, On the numerical detection of the effective stability of chaotic motions in quasi-integrable systems. Physica D, 163, 1-2: 1-25 (2002).

[14] Guzzo M. and Lega E., The numerical detection of the Arnold web and its use for long–term diffusion studies in conservative and weakly dissipative systems, Chaos 23, article 023124, 2013.

[15] Haller G., Lagrangian Coherent Structures. Annual Rev. Fluid. Mech, 47, 137-162, published online, 2014.

[16] Kazimirchak-Polonskaya, E. I., Evolution of Short-Period Comet Orbits from 1660 to 2060, and the Role of the Outer Planets. Soviet Astronomy, Vol. 11, p.349m 1967.

[17] Kazimirchak-Polonskaya, E. I., Review of investigations performed in the USSR on close approaches of comets to Jupiter and the evolution of cometary orbits. In NASA. Goddard Space Flight Center The Study of Comets, Part 1 p 490-536, 1976.

[18] Królikowska M., 67P/Churyumov-Gerasimenko – potential target for the Rosetta mission, Acta Astronomica, vol 53, 195-209, 2003.

[19] Lega E., Guzzo M. and Froeschlé C. Close encounters and resonances detection in three body problems through Levi-Civita regularization. MNRAS, 418, 107-113, 2011.

[20] Marsden B. G., Sekanina Z., and Yeomans D. K., Comets and nongravitational forces. V. Astron. J., 78, 211–225, 1973.

[21] Shadden, S. C., Lekien, F. and Marsden, J. E., Definition and properties of Lagrangian coherent structures from finite-time Lyapunov exponents in two-dimensional aperiodic flows, Physica D, 212(3-4), 271-304, 2005.

[22] Sierks H. et al., On the nucleus structure and activity of comet 67P/Churyumov-Gerasimenko, Science, vol. 347, issue 6220, 2015.

[23] Valsecchi G.B., Manara A., Dynamics of comets in the outer planetary region, II. Enhanced planetary masses and orbital evolutionary paths. Astron. Astrophys. 323, 986–998, 1997.

[24] Yeomans, D. K., Chodas, P. W., Sitarski, G.; Szutowicz, S., Królikowska, M., Comets II, M. C. Festou, H. U. Keller, and H. A. Weaver (eds.), University of Arizona Press, Tucson, 745 pp., p.137-151, 2004.